Journal of Power Sources 244 (2013) 101–108

Contents lists available at SciVerse ScienceDirect

Journal of Power Sources

journal homepage: www.elsevier.com/locate/jpowsour

A simulation on safety of $LiFePO_4$/C cell using electrochemical–thermal coupling model

Songrui Wang, Lili Lu, Xingjiang Liu*

Science and Technology on Power Source Laboratory, Tianjin Institute of Power Sources, Tianjin, China

HIGHLIGHTS

- A electrochemical–thermal coupling model for $LiFePO_4$/C cells was developed.
- Thermal behaviors of $LiFePO_4$/C cells were simulated.
- Inner short circuit or decomposition reactions is major factor of the cell's safety

ARTICLE INFO

Article history:
Received 28 November 2012
Received in revised form
25 February 2013
Accepted 8 March 2013
Available online 25 March 2013

Keywords:
Lithium iron phosphate cell
Electrochemical–thermal model
Separator
Safety

ABSTRACT

An electrochemical–thermal coupling model for $LiFePO_4$/C cells is developed by combining White's electrochemical model with thermal model. And the simulations on thermal behavior of $LiFePO_4$/C cells present the entire process from self-heating to thermal runaway, as well as heating sources at each stage based on DSC data. $LiFePO_4$/C cells, using separator with different melting-down temperature have been simulated, and the results show that the inner short circuit, caused by the melting down of separator, is the major factor of thermal runaway of $LiFePO_4$/C cell, in which the separator with lower melting-down temperature has been used. However, when the $LiFePO_4$/C cell employs a separator with higher melting-down temperature, decomposition reactions of electrodes material become the major factor of the safety.

1. Introduction

Lithium-ion batteries have been widely applied in many fields, including automobile and large-scale power storage. But their applications have been restricted by potential risk of exploding. Mathematic simulations on thermal behavior of lithium ion cells are helpful to designers for understanding the principle and mechanism about safety of lithium ion cells. As well known, there are two kinds of mathematic model of lithium ion cells: thermal model [1–12] and electrochemical model [13–17]. The former one, based on reactions of materials, energy balance and other equations, can be used to simulate thermal stability of cells and investigate their safety. The latter one, based on electrochemical theories, parameters of materials, cell structure and other equations describing relative physical phenomena, can be used to simulate cells performance and investigate the relationship between cell chemistry, structure, capacity and electrochemical performance. The total heat generation from lithium ion cells can usually be divided into two parts. One is caused from the decomposition of materials, which can be simulated by thermal model. Another is caused from the thermal efficiency during charge–discharge, which can be simulated by electrochemical model. Therefore, thermal behavior of lithium ion cells can be simulated by coupling electrochemical model with thermal model.

The $LiFePO_4$ is one of the most attractive cathode materials in mobile and large-scale energy storage, due to excellent thermal safety, low toxicity, low cost, and environmental friendliness [18,19]. Many efforts have been done to improve the thermal stability of $LiFePO_4$/C cells, including improvements of materials, factors of electrodes and designs of $LiFePO_4$/C cells [20,21]. However, $LiFePO_4$/C cells might be in the risk of accidents in the severe conditions.

In this paper, electrochemical–thermal coupling model was constructed and applied to simulate the thermal behavior of $LiFePO_4$/C cells. And the safety performance of $LiFePO_4$/C cell was investigated using simulation based on the coupling model.

* Corresponding author.
E-mail address: klpsc@yahoo.com.cn (X. Liu).

0378-7753/$ – see front matter © 2013 Elsevier B.V. All rights reserved.
http://dx.doi.org/10.1016/j.jpowsour.2013.03.100

Table 1
The equations used in electrochemical–thermal model.

Process	Equations
Current balance (φ_1 solid-phase potential)	$\nabla(-\kappa_1^{\text{eff}}\nabla\varphi_1) = -S_a i_{\text{loc}}, \kappa_1^{\text{eff}} = \kappa_1\varepsilon_1^{\gamma}$
Ion charge balance ($\varphi_2$liquid-phase potential)	$\nabla\left[-\kappa_2^{\text{eff}}\nabla\varphi_2 + \frac{2RT\kappa_2^{\text{eff}}}{F}\left(1+\frac{\partial \ln f}{\partial \ln c_2}\right)(1-t_+)\nabla(\ln c_2)\right] = S_a i_{\text{loc}},$ $\kappa_2^{\text{eff}} = \kappa_2\varepsilon_2^{\gamma}, \frac{\partial \ln f}{\partial \ln c_2} = 0$
Solid state diffusion (c_1 solid-phase concentration)	$\frac{\partial c_1^{\text{ave}}}{\partial t} = -\frac{3S_a i_{\text{loc}}}{F} + R_i c_1^{\max}, c_1^{\text{ave}} - c_1 = \frac{i_{\text{loc}} r_p}{5FD_1}, x = \frac{c_1}{c_1^{\max}}$
Liquid phase diffusion (c_2 liquid-phase concentration)	$\varepsilon_2\frac{dc_2}{dt} + \nabla(-D_2^{\text{eff}}\nabla c_2) = \frac{S_a i_{\text{loc}}}{F}(1-t_+) + 1000\varepsilon_2 R_{\text{ele}}, \quad D_2^{\text{eff}} = D_2\varepsilon_2^{\gamma}$
Butler–Volmer (U equilibrium potential)	$i_{\text{loc}} = kc_2^{\alpha_a}(c_1^{\max}-c_1)^{\alpha_a}c_1^{\alpha_c}$ $\left\{\exp\left[\frac{\alpha_a F}{RT}(\varphi_1-\varphi_2-U)\right] - \exp\left[-\frac{\alpha_c F}{RT}(\varphi_1-\varphi_2-U)\right]\right\}$
$LiFePO_4$ decomposition (x in Li_xFePO_4)	$R_i = A_{\text{pos}}\exp\left[\frac{-E_{\text{apos}}}{RT}\right]x_{\text{pos}}^{n_{\text{pos}}}(1-x_{\text{pos}})^{a_{\text{pos}}}$
Carbon decomposition (x in Li_xC_6)	$R_i = -A_{\text{neg}}\exp\left[\frac{-E_{\text{aneg}}}{RT}\right]x_{\text{neg}}^{n_{\text{neg}}}(1-x_{\text{neg}})^{a_{\text{neg}}}$
Electrolyte decomposition (c_2 liquid-phase concentration)	$R_{\text{ele}} = -A_{\text{ele}}\exp\left[\frac{-E_{\text{aele}}}{RT}\right]x_2^{n_{\text{ele}}}\lvert 1-x_2\rvert^{a_{\text{ele}}}, x_2 = \frac{c_2}{1000}$
SEI decomposition/gasifying/ solvent decomposition	$R_x = -A_x\exp\left[\frac{-E_{ax}}{RT}\right]x_x^{n_x}(1-x_x)^{a_x}$
Thermal diffusion	$\rho C_p\frac{\partial T}{\partial t} - \nabla(K\nabla T) = Q$
Energy balance	$Q = S_a i_{\text{loc}}(\varphi_1-\varphi_1-U) + S_a i_{\text{loc}}T\frac{\partial U}{\partial T} + \kappa_1^{\text{eff}}\nabla\varphi_1\cdot\nabla\varphi_1 + \kappa_2^{\text{eff}}\nabla\varphi_2\cdot\nabla\varphi_2 + \frac{2RT\kappa_2^{\text{eff}}}{F}\left(1+\frac{\partial \ln f}{\partial \ln c_2}\right)(1-t_+)\nabla(\ln c_2)\cdot\nabla\varphi_2 + \sum_i\lvert H_i\rho_i R_i\rvert$

2. Experimental

CR2430 coin cells, with lithium foil as counter electrode and 1 M $LiPF_6$ in EC:DEC:DMC (1:1:1 in volume) as electrolyte, were assembled to test the equilibrium potential of $LiFePO_4$ and carbon materials at different states of charge. C/20 current rate was used to reach preconcerted states of charge, and the potential was recorded after 15 min at each preconcerted state of charge. In addition, the entropy changes of $LiFePO_4$ and carbon materials at different states of charge were tested from 25 °C to 55 °C.

Table 2
The parameters used in electrochemical–thermal model of $LiFePO_4$/C cells.

	$LiFePO_4$	Carbon	Electrolyte
Electric conductivity κ_1/S m^{-1}	51.8	300	–
Solid phase vol-fraction ε_1	0.357	0.528	–
Specific surface area S_a/m^2 m^{-3}	2.434×10^6	4.526×10^6	–
Electrolyte phase vol-fraction ε_2	0.384	0.3	1 (Sep)
Max solid phase concentration $c_1^{\max}$/mol m^{-3}	17623.24	25969.33	–
Particle radius r_p/m	4.4×10^{-7}	3.50×10^{-7}	–
Li-diffusivity D/m^2 s^{-1}	4.27×10^{-14}	2.06×10^{-13}	7.50×10^{-11}
Electrochemical reaction rate coefficient k	5.913×10^{-6}	4.064×10^{-5}	–
dU/dT/V K^{-1}	0.00037 (0.99[a]) 0.00013 (0.85[a]) 8.82×10^{-5} (0.56[a]) 0.000102 (0.38[a]) 0.00014 (0.26[a])	0.00076 (0.04[a]) 0.000219 (0.21[a]) −0.00018 (0.37[a]) −0.00012 (0.51[a])	–
Density ρ/kg m^{-3}	1975	1455	1009
Specific heat Cp/J (kg K)$^{-1}$	1369.21	1437.4	1978.16
Thermal conductivity K/W (m K)$^{-1}$	1.58	1.04	0.33
Initial concentration c_0	$Li_{0.18}FePO_4$	$Li_{0.5}C_6$	1×10^3 mol m^{-3}
Cationic transport number t_+	0.363 [14]	0.363 [14]	0.363 [14]
Bruggemann coefficient γ	1.5 [14]	1.5 [14]	–
Frequency factor A	2.0×10^8	7.76×10^{15} 2.34×10^6 (SEI)	2.0×10^5 1.2×10^9 (Gas) 7.4×10^5 (Sol)
Activation energy Ea/J mol^{-1}	1.03×10^5	1.88×10^5 6.92×10^4 (SEI)	7.58×10^4 1.05×10^5 (Gas) 1.10×10^5 (Sol)
Reaction order n	1.92	0.85 1.79 (SEI)	1.47 1 (Gas) 0.92 (Sol)
Reaction order a	0.67	0 0 (SEI)	0.4 0.71 (Gas) 0.16 (Sol)
Heat H/J g^{-1}	194.7	447.1 300.2 (SEI)	311 −88.3 (Gas) 608 (Sol)

[a] x in Li_xFePO_4 or Li_xC_6.

DSC samples were prepared by putting fully charged $LiFePO_4$ materials/carbon materials with electrolyte into sealed stainless crucibles, which could stand as high pressure as 100 bar. And all operations were done in a glove box filled with Ar. DSC measurements were carried out on Netzsch 204 F1, in a temperature range of 50–490 °C, at different scan rates of 5 °C min^{-1}, 10 °C min^{-1} and 15 °C min^{-1}, respectively.

AC impedance measurements were performed using the Solartron Analytical 1400–1470E CellTest System. Electrochemical impedance spectrum (EIS) was used to calculate the constants of electrochemical reaction rate and the diffusion coefficients of $LiFePO_4$ and carbon materials [22,23]. Three-electrode systems were assembled with either $LiFePO_4$ materials or carbon materials as working electrode, lithium metal as reference and counter electrode. Potential step chronoamperometry [24,25] was also carried out, using a step of 100 mV.

3. Simulation model

Electrochemical model, proposed by R. E. White in 2008 [4], and thermal model, based on reactions tested by DSC [26–28], were coupled in thermal balance of cells and in lithium concentration of $LiFePO_4$, carbon and electrolyte. Equations, describing other physical and chemical phenomena, such as liquid-phase and solid-phase potential, Butler–Volmer electrode kinetics and decomposition of SEI film, were hypothesized as same as those in electrochemical model or thermal model, respectively. A summary of the governing equations and parameters used in this work are listed in Tables 1 and 2, and the equilibrium potential curves are shown in Fig. 1.

COMSOL Multiphysics software was employed to simulate the $LiFePO_4$/C cells using PDE modes, diffusion modes, heat modes and AC/DC modes. All equations were coupled and calculated at the same time in this software.

The simulations on thermal behavior of $LiFePO_4$/C cells were carried out on a simple two-dimension structure model. And there were several hypotheses in the model: $LiFePO_4$/C cells were fully charged. The boundary conditions were hypothesized as adiabatic environment and the initial temperature was set at 398 K (125 °C). The melting-down temperatures of separator were hypothesized as 413 K (140 °C), 433 K (160 °C), 453 K (180 °C), 473 K (200 °C), 493 K (220 °C), and 513 K (240 °C), respectively. Separator had been melt-down completely at hypothesized temperature and separator shrinkage before melting down was ignored due to uncertainty. After melting-down completely, the electric conductivity of separator was hypothesized as same as that of $LiFePO_4$ electrode. The heat consumed during melting-down of separator was ignored.

4. Results and discussion

Fig. 2 shows the simulation results of $LiFePO_4$/C cell using separator with melting-down temperature at 453 K (180 °C). The self-heating of $LiFePO_4$/C cell was investigated, staring at 398 K (125 °C) in an adiabatic environment. There are three stages in temperature/heating rate curves (Fig. 2a). Before 419 K (146 °C), the temperature of cell increases with a rate, from 0.011 K s^{-1} to 0.0022 K s^{-1}, and it needs 3580 s in this stage. From 419 K (146 °C) to 453 K (180 °C), the temperature of cell increases smoothly. After the temperature reaches 453 K (180 °C), the separator melting-down temperature, the heating rate increases quickly from 0.005 K s^{-1} to 0.04 K s^{-1} and the temperature of cell reaches 461 K (188 °C) in about another 900 s. And then the heating rate reaches as high as 0.6 K s^{-1} in about 137 s, and $LiFePO_4$/C cell goes into thermal runaway. Compared with material reactions rates in Fig. 2b, it is found that the temperature of cell increases during the first stage in temperature curve, because of the heat from the decomposition of SEI film. And when the temperature of cell reaches 419 K (146 °C), SEI film has been exhausted, some solvents start to gasify, which is an endothermic process, and exothermic reaction of electrolyte is also going on. Thus the temperature of cell increases smoothly during this period. After 440 K (167 °C), the $LiFePO_4$ electrode begins to decompose, which accelerates the temperature increasing. When the temperature of cell is higher than the separator melting-down temperature, 453 K (180 °C), inner short circuit appears, and accelerates the reaction rates of $LiFePO_4$ electrode, carbon electrode and electrolyte. Temperature and heating rate are led to acute increasing due to the thermal efficiency. Then $LiFePO_4$/C cell goes into thermal runaway in a few seconds.

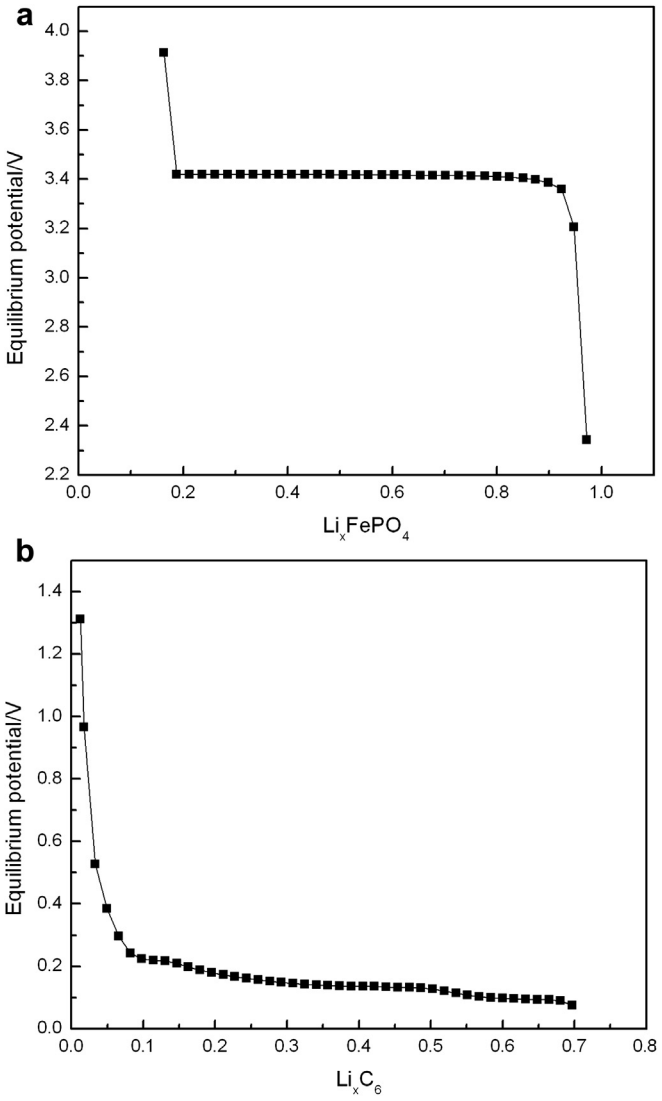

Fig. 1. The equilibrium potential curves of $LiFePO_4$ electrode (a) and carbon electrode (b).

When the melting-down temperature of separator is defined as high as 513 K (240 °C), the simulated results are shown in Fig. 3. Before the temperature of cell reaches 453 K (180 °C), the curves of temperature, heating rate and reactions rates are as same as those in Fig. 2. After that, without inner short circuit, the temperature of cell still increases smoothly, due to decomposition of $LiFePO_4$ electrode. When the temperature of cell reaches 469 K (196 °C), the carbon electrode also begins to decompose. Thus the heating rate becomes stepped-up. It needs 2440 s for the temperature of

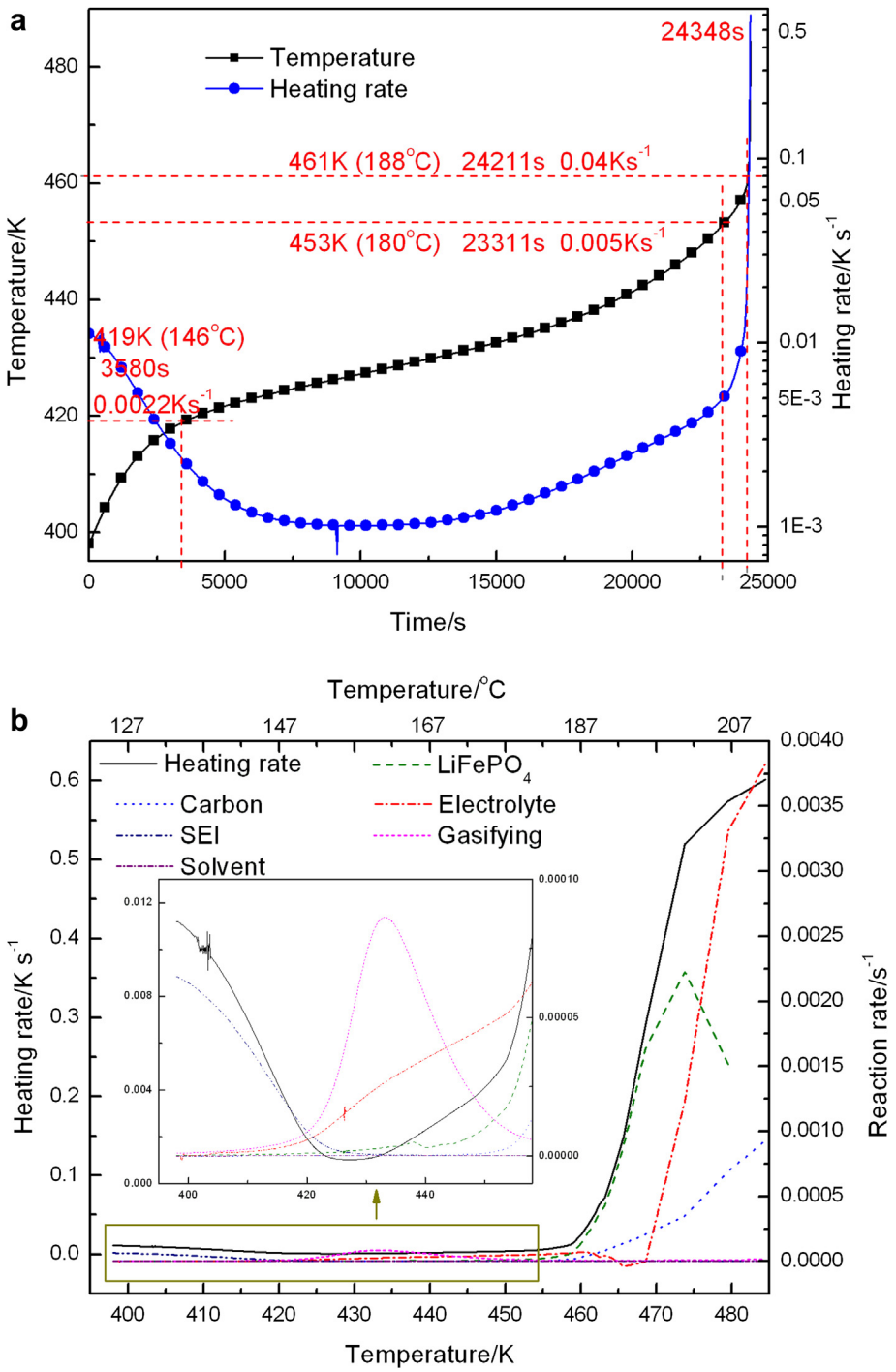

Fig. 2. The simulation results of $LiFePO_4$/C cells using separator with melting temperature at 453 K, a: the simulation results of temperature and heating rate curves; b: the simulation results of reactions rates. ($LiFePO_4$/C cells were fully charged, the boundary conditions were adiabatic environment and the initial temperature was 398 K (125 °C.))

$LiFePO_4$/C cell range from 453 K (180 °C) to 469 K (196 °C), at a heating rate of 0.01 K s^{-1}, and another 1190 s are needed for the heating rate to reach 0.04 K s^{-1}, which is much longer than that in Fig. 2. Finally, $LiFePO_4$/C cell goes into thermal runaway, in 308 s with a rate as high as 0.22 K s^{-1}, much lower than 0.6 K s^{-1} in Fig. 2. From simulation results, it is clear that the thermal runaway of $LiFePO_4$/C cell should be caused by decompositions of $LiFePO_4$ and carbon electrodes. $LiFePO_4$/C cell, using separator melting-down at 513 K (240 °C), has shown better thermal stability than that using separator melting-down at 453 K (180 °C).

Thermal behaviors of $LiFePO_4$/C cells using separator with different melting-down temperature, have been simulated, and the results are shown at Fig. 4. $LiFePO_4$/C cell using separator with higher melting-down temperature, goes into thermal runaways at higher temperature, until the separator melting temperature reaches 493 K (220 °C). From this result, it can be deduced that the thermal safety of $LiFePO_4$/C cell, using separator with melting-down temperature lower than 493 K (220 °C), is determined by inner circuit, which is caused by the melting down of the separator. That means the melting-down temperature of separator is the

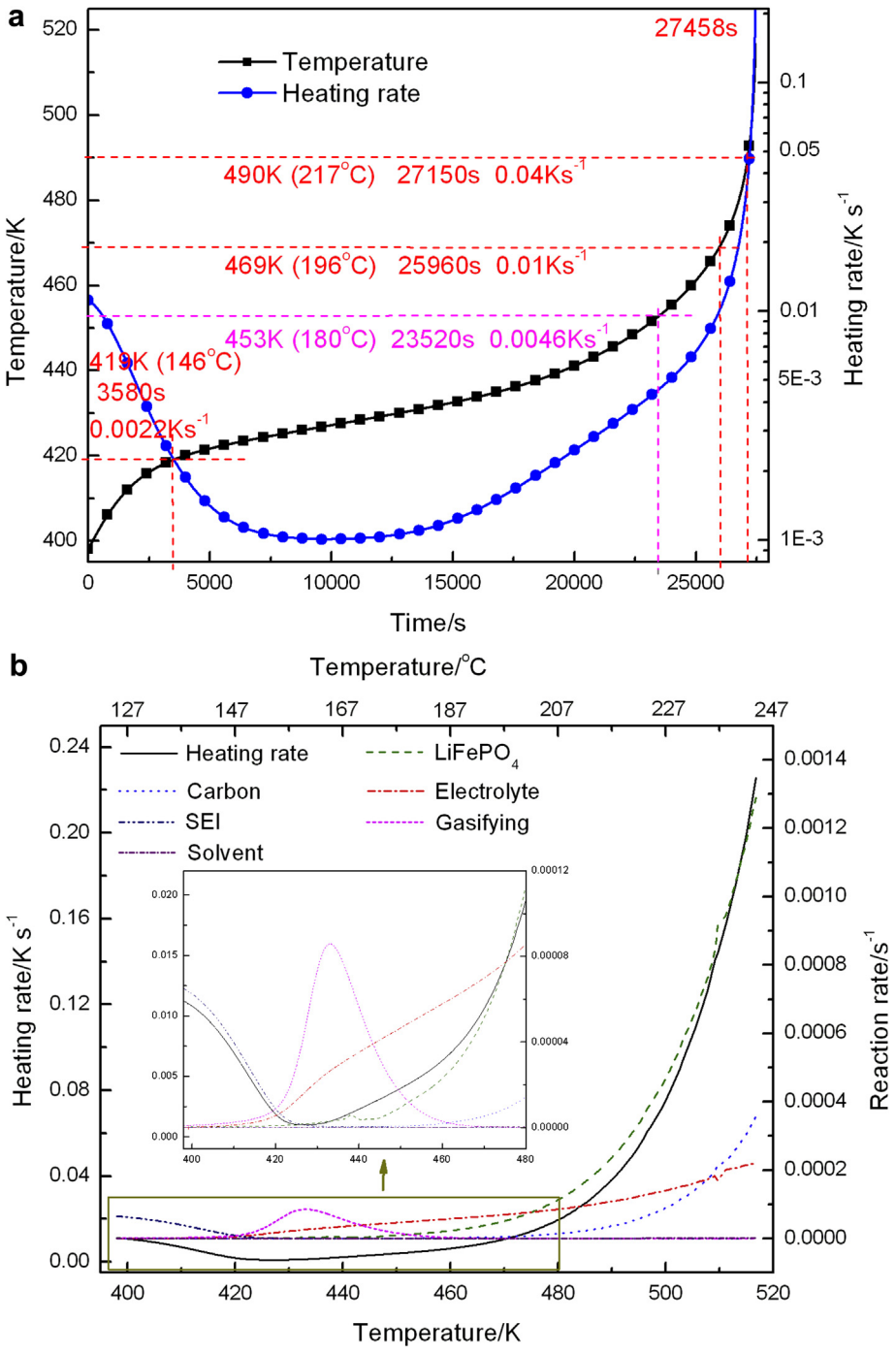

Fig. 3. The simulation results of $LiFePO_4$/C cells using separator with melting temperature at 513 K, a: the simulation results of temperature and heating rate curves; b: the simulation results of reactions rates. ($LiFePO_4$/C cells were fully charged, the boundary conditions were adiabatic environment and the initial temperature was 398 K (125 °C.))

major factor of thermal safety of $LiFePO_4$/C cell. In this case, the temperature of $LiFePO_4$/C cell increase because of the heat released from decomposition of SEI film, gasification of solvents in electrolyte, and decomposition of electrolyte, $LiFePO_4$ electrode and carbon electrode. When the temperature reaches the melting-down temperature of separator, inner short circuit happens due to the melting down of the separator, and the temperature of $LiFePO_4$/C cell increases rapidly because of such great joule heat from short circuit. And then the $LiFePO_4$/C cell soon goes into thermal runaway.

However, the thermal stability of $LiFePO_4$/C cell, using separator with the melting-down temperature higher than 493 K (220 °C), depends on the decomposition of electrodes materials. And the heating rate of $LiFePO_4$/C cell is determined by electrodes decomposition rates, and is much lower than that caused by inner short circuit.

Furthermore, the reaction rates of $LiFePO_4$ electrode and carbon electrode are also shown in Fig. 5. The reaction rate is the summation of electrochemical reaction rate and decomposing reaction rate. For $LiFePO_4$/C cell, using separator with lower melting-down

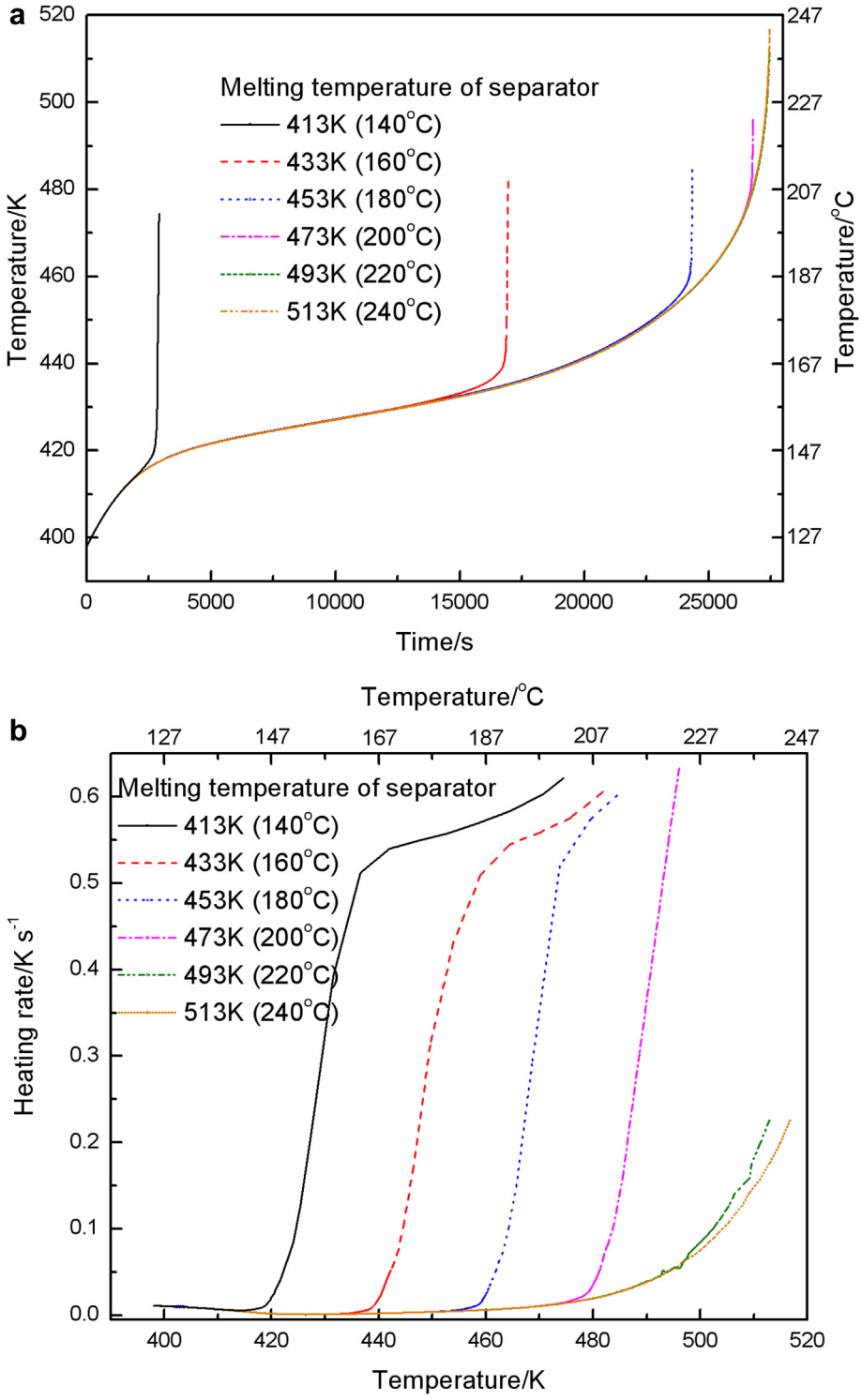

Fig. 4. The simulation results of $LiFePO_4$/C cells using separator with different melting temperature, a: the simulation results of temperature curves; b: the simulation results of heating rate curves. ($LiFePO_4$/C cells were fully charged, the boundary conditions were adiabatic environment and the initial temperature was 398 K (125 °C.))

temperature, such as 413 K (140 °C), 433 K (160 °C), when the temperature of $LiFePO_4$/C cell reaches the melting-down temperature of separator, inner short circuit occurs and electrochemical reactions of electrodes take place rapidly, thus the rates of $LiFePO_4$ and carbon electrodes reactions increase sharply. With electrochemical reactions going on for a period, the surface concentrations of reactants decrease, and the rates of electrochemical reactions decrease. At the same time, the temperature of $LiFePO_4$/C cell increases because of the heat accumulating and reaches the temperature of electrodes decompositions, and then the rates of electrodes reactions increase sharply again.

For $LiFePO_4$/C cell, using separator with a little higher melting-down temperature, such as 453 K (180 °C), 473 K (200 °C), when the temperature of $LiFePO_4$/C cell reaches the melting-down temperature of separator, decomposition reactions of electrodes take place also. Electrochemical reactions, caused by inner short circuit,

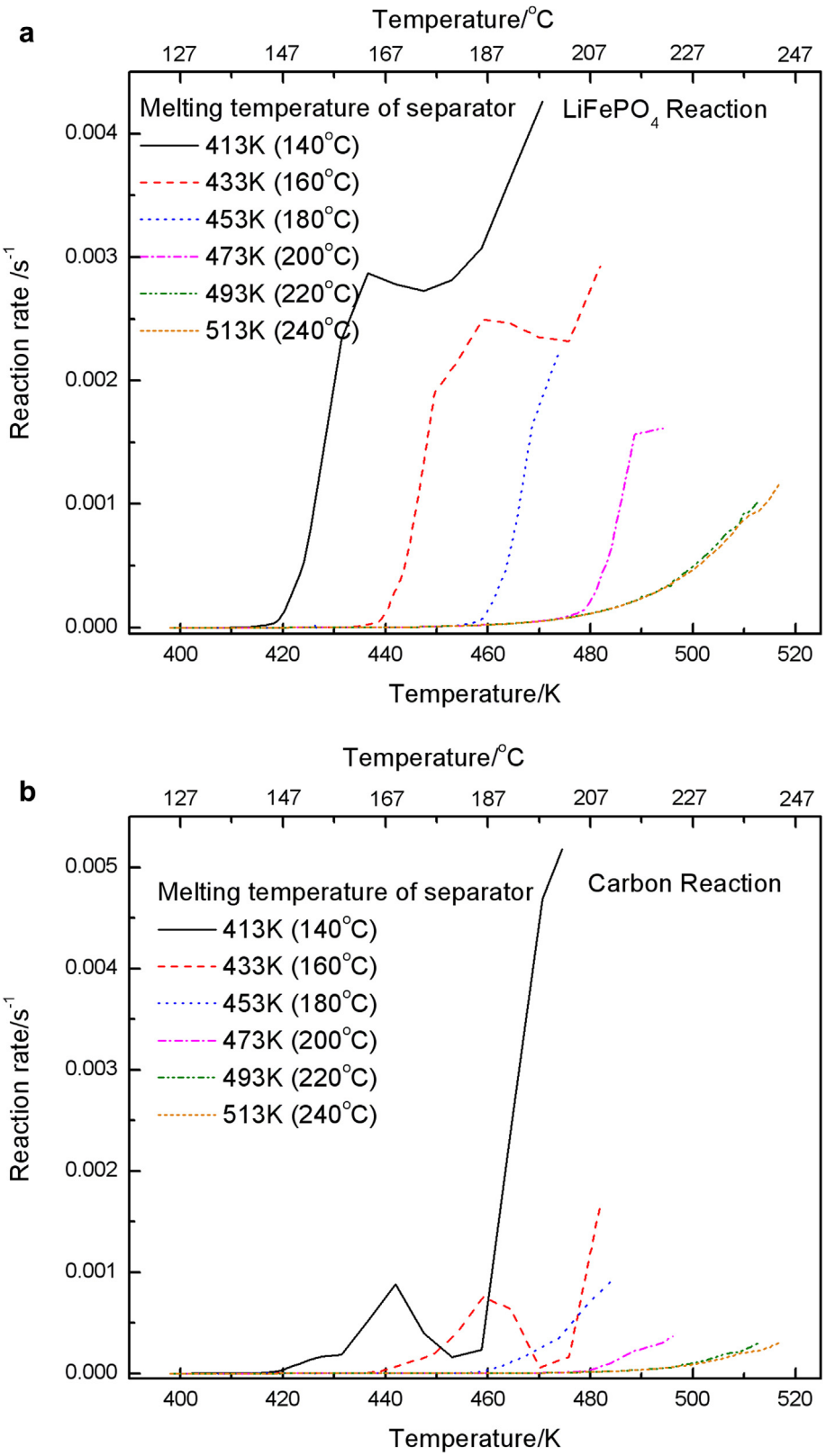

Fig. 5. The simulation results of reactions rates in $LiFePO_4$/C cells using separator with different melting temperature, a: the simulation results of $LiFePO_4$ electrode reactions; b: the simulation results of carbon electrode reactions. ($LiFePO_4$/C cells were fully charged, the boundary conditions were adiabatic environment and the initial temperature was 398 K (125 °C.))

and decomposition reactions go on at the same time, and the rates of electrodes reactions increase sharply.

For $LiFePO_4$/C cell, using separator with highest melting-down temperature, such as 493 K (220 °C), 513 K (240 °C), the rates of electrodes reactions are mainly dominated by decomposition reactions.

5. Conclusion

Electrochemical–thermal coupling model was used to investigate the safety of $LiFePO_4$/C cells, using separator with different melting-down temperature. The results show that: the safety of $LiFePO_4$/C cells depends on both inner short circuit and decomposition reactions of electrodes. When separator with higher melting-down temperature is used in $LiFePO_4$/C cell, decomposition reactions of electrodes materials play a most important role in thermal runaway of $LiFePO_4$/C cell. However, when separator with lower melting-down temperature is used in $LiFePO_4$/C cell, inner short circuit, caused by the melting down of the separator, is the major factor of thermal runaway of the $LiFePO_4$/C cell. In the latter case, the process could be described as: the temperature of $LiFePO_4$/C cell increases because of heat generating from decomposition of SEI film, gasification of solvents in electrolyte, and decomposition of electrolyte, $LiFePO_4$ electrode and carbon electrode, until it reaches the melting-down temperature of separator. Then inner short circuit occurs, caused by the melting down of separator, and $LiFePO_4$/C cell goes into thermal runaway due to great joule heat from inner short circuit.

References

[1] T.D. Hatchard, D.D. Macneil, J.R. Dahn, J. Electrochem. Soc. 148 (2001) A755–A761.
[2] G.H. Kim, A. Pesaran, R. Spotnitz, J. Power Sources 170 (2007) 476–489.
[3] D.D. MacNeil, J.R. Dahn, J. Phys. Chem. 105 (2001) 4430–4439.
[4] P.G. Balakrishnan, R. Ramesh, T.P. Kumar, J. Power Sources 155 (2006) 401–414.
[5] Q.S. Wang, P. Ping, J.H. Sun, Nonlinear Dyn. 61 (2010) 763–772.
[6] Y.F. Chen, J.W. Evans, J. Electrochem. Soc. 143 (1996) 2708–2712.
[7] D.H. Doughty, P.C. Butler, R.G. Jungst, E.P. Roth, J. Power Sources 110 (2002) 357–363.
[8] Q.S. Wang, J.H. Sun, X.F. Chen, G.Q. Chu, C.H. Chen, Mater. Res. Bull. 44 (2009) 543–548.
[9] J. Yamaki, Y. Baba, N. Katayama, H. Takatsuji, M. Egashira, S. Okada, J. Power Sources 119 (2003) 789–793.
[10] Y.F. Chen, J.W. Evans, J. Electrochem. Soc. 141 (1994) 2947–2955.
[11] G.F. Guo, B. Long, B. Cheng, S.Q. Zhou, P. Xu, B.G. Cao, J. Power Sources 195 (2010) 2393–2398.
[12] Q. Wang, P. Ping, X. Zhao, G. Chu, J. Sun, C. Chen, J. Power Sources 208 (2012) 210–224.
[13] K. Kumaresan, G. Sikha, R.E. White, J. Electrochem. Soc. 155 (2008) A164–A167.
[14] M. Doyle, J. Newman, A.S. Gozdz, J. Electrochem. Soc. 143 (1996) 1890–1903.
[15] T.F. Fuller, M. Doyle, J. Newman, J. Electrochem. Soc. 141 (1994) 1–9.
[16] Q. Zhang, Q. Guo, R.E. White, J. Power Sources 165 (2007) 427–435.
[17] W.B. Gu, C.Y. Wang, J. Electrochem. Soc. 147 (2000) 2910–2922.
[18] X.Z. Liao, Y.S. He, Z.F. Ma, X.M. Zhang, L. Wang, J. Power Sources 174 (2007) 720–725.
[19] T. Shiratsuchi, S. Okada, J. Yamaki, S. Yamashita, T. Nishida, J. Power Sources 173 (2007) 979–984.
[20] H. Liu, G.X. Wang, D. Wexler, J.Z. Wang, H.K. Liu, Electrochem. Commun. 10 (2008) 165–169.
[21] M. Koltypin, D. Aurbach, L. Nazar, B. Ellis, Eletrochem. Solid-State Lett. 10 (2007) A40–A44.
[22] Z. Yang, Y. Feng, Z. Li, S. Sang, Y. Zhou, L. Zeng, J. Electroanal. Chem. 580 (2005) 340–347.
[23] R.B. Hadlean, J. Farcy, J.P.P. Ramos, N. Baffler, J. Electrochem. Soc. 143 (1996) 2083–2088.
[24] H. Sato, D. Takahashi, T. Nishina, I. Uchida, J. Power Sources 68 (1997) 540–544.
[25] F. Feng, J. Han, M. Geng, D.O. Northwood, J. Electroanal. Chem. 487 (2000) 111–119.
[26] S.R. Wang, L.L. Lu, X.J. Liu, 2010 China–Korea Lithium Battery Workshop, Guangzhou, 2010, pp. 144–159.
[27] S.R. Wang, L.L. Lu, X.J. Liu, The 62nd Annual Meeting of the International Society of Electrochemistry, Niigata, 2011, S06-P-023 (ise111042).
[28] S.R. Wang, L.L. Lu, X.J. Liu, Chin. J. Power Sources 34 (2010) 41–44.